Vol 16 No 9, September 2007
1009-1963/2007/16(09)/2537-07

Chinese Physics

© 2007 Chin. Phys. Soc.
and IOP Publishing Ltd

Exciton–polaritons in ternary mixed crystals*

Liu Li(刘 丽), Liang Xi-Xia(梁希侠)†, and Bao Jin(包 锦)

Department of Physics, Inner Mongolia University, Hohhot 010021, *China*

(Received 8 October 2006; revised manuscript received 30 January 2007)

In this paper the bulk exciton polaritons in ternary mixed crystals (TMCs) are investigated in the Born–Huang approximation. The numerical results of the polariton frequencies as functions of the wave-vector and the compositions for ternary mixed crystals $Al_xGa_{1-x}As$, $Cd_xZn_{1-x}Se$, and $Al_xGa_{1-x}N$ are obtained and discussed. The new dispersion characteristics for exciton–polaritons in TMC systems are found in comparison with binary crystals. The splitting of the two branches of exciton–polariton frequencies varies nonlinearly with the composition of TMCs and has a minimum in the long-wavelength range.

Keywords: polariton, exciton, ternary mixed crystal
PACC: 0350D, 7135, 6350

1. Introduction

Exciton–polaritons, as a kind of mixed mode of elementary excitations in condensed matter, have attracted a great deal of interest since the pioneering work of Hopfield *et al.*[1−3] Properties of exciton–polaritons associated with transverse excitons coupled to electromagnetic waves have been successfully studied experimentally and theoretically.[4−7] Exciton–polaritons have been first observed experimentally by the methods of resonant Brillouin scattering (RBS) and two-photon resonant Raman scattering (RRS).[3,8,9] Later, the exciton–polaritons in quantum-confined systems, such as quantum wells,[10,11] superlattices,[5,12] microcavities[4,6,7] and other systems,[13−15] were also studied. Very recently, the spin dynamics, photoluminescence dynamics and nonequilibrium Bose–Einstein condensation of exciton–polaritons have been extensively investigated experimentally by various optical methods.[16,17]

In recent years, the properties of ternary mixed crystals (TMCs) have attracted much attention of both theoretical and experimental scientists,[18−20] because of their increasing role for the development of optoelectronic devices. As is well known, an important feature of TMCs, which is quite different from binary crystals, is that the band structure can be varied over a wide range by altering the composition of the alloys. Excitons and related elementary excitations play the crucial role for the optical and electrical properties of TMC systems.[19,21] Naturally, the novel properties of excitons in TMCs, such as the concentration dependence of binding energies and longitudinal–transverse energies, contribute new characteristics of exciton–polaritons. Application of polar TMCs in artificial materials can enable one to modify optical properties of the systems in a controlled manner, and extend their applications to devices.[22−24] Seisyan *et al*[20] investigated experimentally the absorption edge spectra and excitonic absorption index of polar TMC $Al_xGa_{1-x}As$ with different compositions and presented evidence for the existence of bulk exciton–polaritons. However, although the exciton–polaritons of polar binary crystals are widely investigated, to the best of our knowledge, the theoretical studies of the exciton–polaritons in polar TMCs have been rarely reported. The further investigations on the properties of exciton–polaritons in TMC systems are therefore required.

In this paper we discuss the bulk exciton–polaritons in TMCs in the Born–Huang approximation.[25] The polariton-frequencies are calculated numerically as functions of the wave-vector and the compositions for several typical TMCs. The dispersion characteristics and their concentration dependence of the bulk exciton–polaritons are discussed in detail.

2. Theory

Now we explore the properties of exciton–polaritons in bulk polar TMCs. Consider an electro-

*Project supported partly by PhD Progress Foundation of Higher Education Institutions of China (Grant No 20040126003) and the Natural Science Foundation of Inner Mongol of China (Grant No 200408020101).
†Corresponding author. E-mail: xxliang@imu.edu.cn

magnetic wave propagated in a polar TMC $A_xB_{1-x}C$ of cubic symmetry, which couples with a transverse polarization wave of excitons and forms exciton–polaritons. For simplicity, the dielectric function $\varepsilon(k, \omega)$ is considered as isotropic for the TMC materials of cubic symmetry. The propagation of exciton–polaritons in the TMC can be described by linking the Maxwell's equations with the Born–Huang-like equations[25] as follows:

$$\nabla \times \boldsymbol{E} = -\mu_0 \frac{\partial \boldsymbol{H}}{\partial t}, \tag{1}$$

$$\nabla \times \boldsymbol{H} = \frac{\partial}{\partial t}(\varepsilon_0 \boldsymbol{E} + \boldsymbol{P}), \tag{2}$$

$$\nabla \cdot (\varepsilon_0 \boldsymbol{E} + \boldsymbol{P}) = 0, \tag{3}$$

$$\nabla \cdot \boldsymbol{H} = 0, \tag{4}$$

$$\ddot{\boldsymbol{W}} = b_{11}\boldsymbol{W} + b_{12}\boldsymbol{E} + D\nabla^2 \boldsymbol{W}, \tag{5}$$

$$\boldsymbol{P} = b_{21}\boldsymbol{W}_+ b_{22}\boldsymbol{E}. \tag{6}$$

Here $\boldsymbol{E}$ and $\boldsymbol{H}$ are respectively the macroscopic electric and magnetic field and $\boldsymbol{P}$ the macroscopic polarization, μ_0 and ε_0 are the vacuum magnetic permeability and the dielectric constant respectively, $\boldsymbol{W} = (\mu^*/\Omega)^{1/2}\boldsymbol{u}$, where $\boldsymbol{u}$ is the relative displacement of the electron and hole related to the polarization, Ω is the primitive cell volume, $\mu^* = m_{\mathrm{e}}^* m_{\mathrm{h}}^*/(m_{\mathrm{e}}^* + m_{\mathrm{h}}^*)$ is the exciton reduce mass and $M^* = m_{\mathrm{e}}^* + m_{\mathrm{h}}^*$ the exciton mass-centre mass, m_{e}^* and m_{h}^* are respectively the effective masses of the electron and hole. Equation (5) differs from the Born–Huang equation corresponding to the long-wavelength optical phonon field by a spatial-dispersion $D\nabla^2\boldsymbol{W}$, where $D = h\omega_{\mathrm{T}}/M^*$, and ω_{T} is the transverse frequency of the uncoupled exciton mode. The dynamical coefficients b_{ij} $(i, j = 1, 2)$ in Eqs.(5) and (6) have been determined by Tilley,[25] and here we use them directly as follows:

$$b_{11} = -\omega_{\mathrm{T}}^2, \quad b_{12} = b_{21} = (S\varepsilon_0)^{1/2},$$
$$b_{22} = [\varepsilon(0) - 1]\varepsilon_0,$$

where $S = 4\pi\beta\omega_{\mathrm{T}}^2$ is the oscillator strength of exciton at the limit of $\omega = 0$ as well as $k = 0$. $\varepsilon(0)$ is the static dielectric constant.

Let us assume that the solutions of Eqs.(1)–(6) have the following form:

$$\boldsymbol{W}, \boldsymbol{p}, \boldsymbol{E}, \boldsymbol{H} \propto \exp[\mathrm{i}(\boldsymbol{k} \cdot \boldsymbol{r} - \omega t)], \tag{7}$$

where ω and $\boldsymbol{k}$ are respectively the frequency and wave-vector of the exciton–polariton. Using the solutions of form (7) in Eqs.(1)–(6), one can obtain the following equation group:

$$\omega\varepsilon_0 E + \omega P - kH = 0, \tag{8}$$

$$kE - \omega\mu_0 H = 0, \tag{9}$$

$$b_{12}E + (b_{11} + \omega^2 - k^2 D)W = 0, \tag{10}$$

$$b_{22}E - P + b_{21}W = 0. \tag{11}$$

The condition of the equation group having the nonzero solutions is that the coefficient determinant vanishes:

$$\begin{vmatrix} \omega\varepsilon_0 & \omega & -k & 0 \\ k & 0 & -\omega\mu_0 & 0 \\ b_{12} & 0 & 0 & b_{11} + \omega^2 - k^2 D \\ b_{22} & -1 & 0 & b_{21} \end{vmatrix} = 0. \tag{12}$$

Calculating the determinant in Eq.(12), we get the implicit dispersion relation of the exciton–polariton in the TMC:

$$\frac{c^2k^2}{\omega^2} = \varepsilon(0) + \frac{S}{\omega_{\mathrm{T}}^2 + Dk^2 - \omega^2}. \tag{13}$$

The implicit dispersion relation obtained here is consistent with that given by the previous works.[2,25] The oscillator strength $S = 4\pi\beta\omega_{\mathrm{T}}^2$ is determined by[26]

$$4\pi\beta = 4\hbar c\varepsilon^{1/2}(0)E_x\alpha(E_{\mathrm{g}})/\pi E_{\mathrm{g}}^2, \tag{14}$$

where E_x is the exciton binding energy and $\alpha(E_{\mathrm{g}})$ the absorption coefficient at the band-gap energy E_{g}, which can be written as[27,28]

$$\alpha(E_{\mathrm{g}}) = \frac{4\pi e^2\hbar}{\varepsilon_0 m_{\mathrm{e}}^{*2}}\Big(\frac{2\mu^*}{\hbar^2}\Big)^{3/2}|P_{\mathrm{CV}}|^2\frac{E_x^{1/2}}{\eta E_{\mathrm{g}}}. \tag{15}$$

Here P_{CV} is the momentum matrix element at $k = 0$ and given by

$$|P_{\mathrm{CV}}|^2 = \frac{E_{\mathrm{g}}m_0^2}{6\bar{m}_{\mathrm{e}}}, \tag{16}$$

with

$$\frac{m_0}{\bar{m}_{\mathrm{e}}} = \frac{m_0}{m_{\mathrm{e}}^*} - 1. \tag{16a}$$

η is the refractive index and m_0 the rest mass of electron.

According to the relation between E_{L} and E_{T}[29]

$$E_{\mathrm{T}} = \frac{1}{1 + 2\pi\beta/\varepsilon(0)}E_{\mathrm{L}},$$

one can obtain the frequency of longitudinal modes at $k = 0$ as

$$\omega_{\mathrm{L}}^2 = \omega_{\mathrm{T}}^2 + \frac{S}{\varepsilon(0)}. \tag{17}$$

Inserting Eq.(17) into Eq.(13), we obtain the implicit dispersion relation

$$\frac{\hbar^2c^2k^2}{E^2} = \varepsilon(0)\Big(1 + \frac{E_{\mathrm{L}}^2 - E_{\mathrm{T}}^2}{E_{\mathrm{T}}^2 + \hbar^2Dk^2 - E^2}\Big), \tag{18}$$

where $E_{\rm L}$ is determined by relation $E_{\rm L} = E_{\rm g} - E_x$.[30]

Some physical parameters of the TMC, such as $m_{\rm e}$, $m_{\rm h}$, E_x, $\varepsilon(0)$, are usually determined by using the macroscopic parameters of the end-member binary crystals AC ($x = 1$) and BC ($x = 0$), according to the formula of linear interpolation

$$T_{A_xB_{1-x}C}(x) = xB_{AC} + (1-x)B_{BC} \equiv a + bx, \quad (19)$$

where T and B stand for the values of the parameter $m_{\rm e}$, $m_{\rm h}$, E_x or $\varepsilon(0)$ for the TMC and the end-member binary crystal AC (x= 1) or BC (x= 0), respectively, and $a \equiv B_{BC}$ and $b = B_{AC} - B_{BC}$.

The band-gap energy $E_{\rm g}$ in TMCs deviates largely from the linear relation of Eq.(19) and has an approximately quadratic dependence on the composition x. The following approximate relation is then approved:

$$E_{\rm g}(A_xB_{1-x}C)(x) = xE_{\rm g}(AC) + (1-x)E_{\rm g}(BC) + C_{A-B}x(1-x) \equiv a + bx + cx^2, \quad (20)$$

where $a = E_{\rm g}(BC)$, $b = E_{\rm g}(AC) - E_{\rm g}(BC) + C_{A-B}$, and $c = -C_{A-B}$. The parameter c is usually called the 'bowing' or nonlinear parameter.

The dispersion of exciton–polaritons in TMCs can be calculated by using Eqs.(13)–(20).

3. Numerical results and discussion

We have performed the numerical computations of the frequencies of bulk exciton–polaritons for several TMCs of III–V, II–VI compound semiconductors with various composition x. As examples, the exciton–polariton dispersion curves for TMC systems $Al_xGa_{1-x}As$, $Cd_xZn_{1-x}Se$, and $Al_xGa_{1-x}N$ are illustrated in Fig.1, where the composition x is chosen successively as 0, 0.15, 1; 0, 0.5, 1; and 0, 0.5, 1 for the three systems respectively. The used parameters in the calculations are listed in Tables 1 and 2.

Table 1. Effective masses of electrons and heavy holes, static dielectric constants, band-gap energies and exciton binding energies for binary materials. m is measured in the electron rest mass, and energy in eV.

material	$m_{\rm e}$	$m_{\rm hh}$	ε_0	$E_{\rm g}$	E_x
GaAs	0.067[a]	0.62[a]	13.18[a]	1.5194[b]	0.0042[b]
AlAs	0.15[a]	0.76[a]	10.06[a]	3.0994[b]	0.0112[b]
ZnSe	0.17[c]	0.6[c]	8.1[c]	2.821[d]	0.019[g]
CdSe	0.13[c]	0.45[c]	9.6[c]	1.765[d]	0.015[g]
AlN	0.33[c]	4.55[e]	8.5[c]	6.1[f]	0.0565[g]
GaN	0.2[c]	2[e]	9.5[c]	3.5[f]	0.0271[g]

[a]Ref.[31], [b]Ref.[32], [c]Ref.[33], [d]Ref.[34], [e]Ref.[35], [f]Ref.[19], [g]$E_x = 13.6\ \mu^*/\varepsilon^2$(eV).

Table 2. Band-gap energies and exciton binding energies for ternary materials. Energy is measured in eV.

material	$E_{\rm g}$	E_x
$Al_xGa_{1-x}As$	$1.5194 + 1.36x + 0.22x^2$[j]	$0.0042 + 0.007x$[j]
$Cd_xZn_{1-x}Se$	$2.821 - 1.386x + 0.33x^2$[k]	$0.019 - 0.004x$[g]
$Al_xGa_{1-x}N$	$3.5 + 1.6x + x^{2f}$	$0.0271 + 0.0294x$[g]

[j]Ref.[36], [k]Ref.[37]

As expected, the dispersion curves of the exciton–polaritons in Fig.1 degenerate respectively to those of the corresponding binary crystals GaAs, ZnSe, and GaN when $x = 0$ and AlAs, CdSe, and AlN when $x = 1$. The theoretical results here for the dispersion curves and the frequencies of the longitudinal-transverse excitons of binary system GaAs, ZnSe and CdSe are in agreement with experiments.[3,38,39]

When the composition x is neither zero nor one, we can find the dispersion characteristics which are different quantitatively from those in binary crystals. Even though there are still two branches of exciton–polariton frequencies in TMCs, the values of the frequencies change obviously with the composition x.

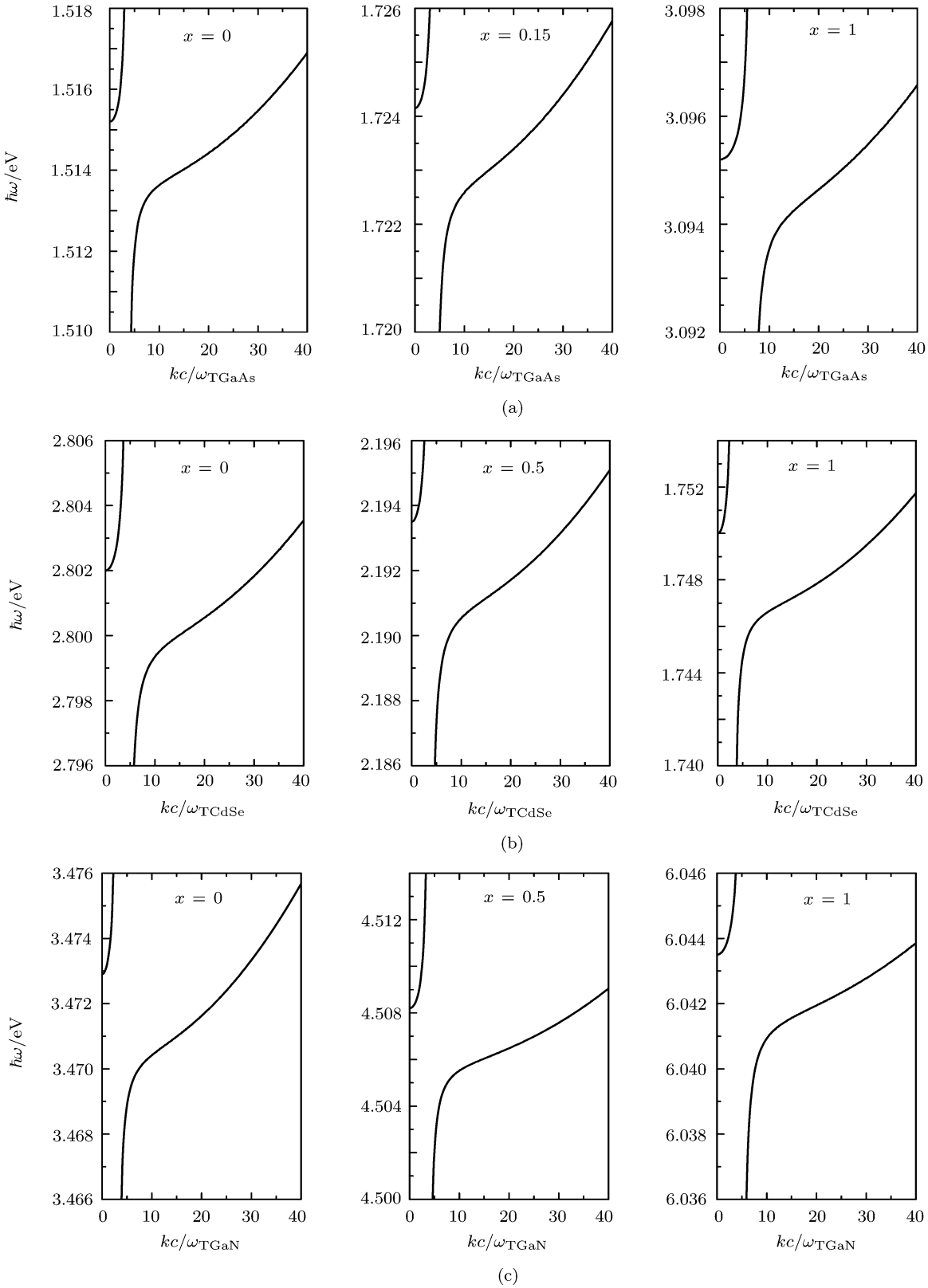


Fig.1. Energies of the bulk exciton–polaritons as functions of the wave-vector for (a) $Al_xGa_{1-x}As$, (b) $Cd_xZn_{1-x}Se$, and (c) $Al_xGa_{1-x}N$. The dimensionless wave-vector kc/ω_{TGaAs}, kc/ω_{TCdSe}, kc/ω_{TGaN} are used, where ω_{TGaAs}, ω_{TCdSe}, and ω_{TGaN} are the frequencies of the uncoupled exciton modes for (a), (b), and (c) respectively, c is the velocity of light.

As $k \to 0$, the upper branch with higher frequencies in the two polariton solutions gets the finite frequency corresponding to the longitudinal exciton of the TMCs (exciton-like behaviour), for which $\varepsilon(k,\ \omega) = 0$. The other one with lower frequencies has vanishing frequency, similar to that in binary system (photon-like behaviour). It is found that the calculated value of the energy (1.7242 eV) of the upper branch of the dispersion curves of TMC $Al_{0.15}Ga_{0.85}As$ at k= 0 in Fig.1(a) agrees very well with the measured value in Ref.[20].

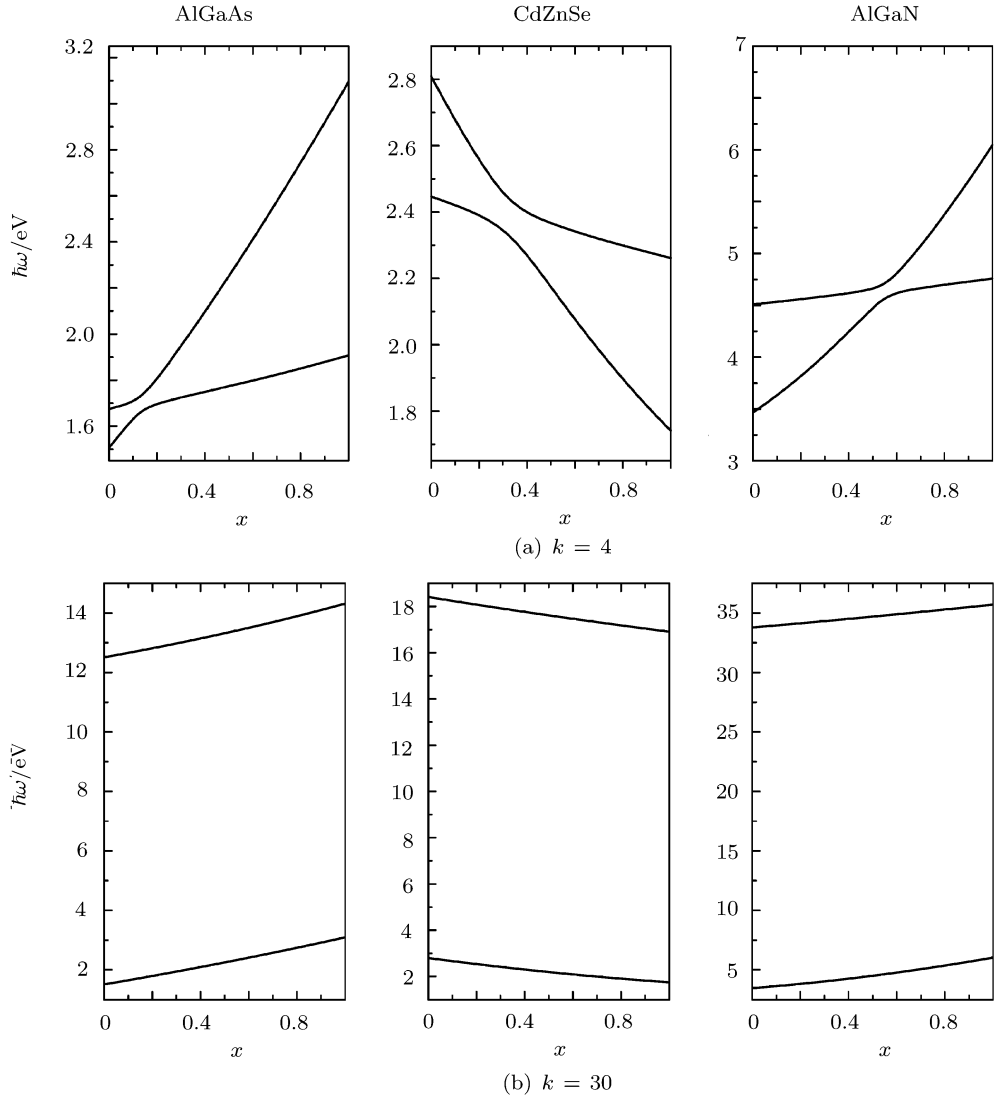


Fig.2. Energies of the exciton–polaritons as functions of the composition x in the TMCs $Al_xGa_{1-x}As$, $Cd_xZn_{1-x}Se$, and $Al_xGa_{1-x}N$ for (a) $k = 4$ and (b) $k = 30$. The wave-vector k is measured in ω_{TGaAs}/c, ω_{TCdSe}/c, and ω_{TGaN}/c respectively.

Along with the increase of the wave-vector k, the frequency of the upper branch of exciton–polaritons increases and rapidly tends to linear (photon-like excitation). Otherwise, the lower branch starts with a photon-like excitation and then turns to an exciton-like excitation at a certain wave-vector (the first knee) with a frequency lower than the transverse-exciton frequency. Next the dispersion curve bends up at a frequency larger than the transverse-exciton frequency (the second knee) due to the spatial dispersion and finally tends to the asymptotic form $E = E_T + h^2k^2/2M^*$ (or $\omega^2 = \omega_T^2 + Dk^2$) as $k \to \infty$. The characteristic of the dispersion curves is similar qualitatively to that in binary crystals, but shows important quantitative difference from binary ones. Most of the characteristic quantities depend on the composition x in TMCs. For example, the positions of the knees in the dispersion curves of exciton-like excitations shift towards the larger wave-vectors with the increase of the mole fraction of the wider band-

gap binary end-materials, i.e. AlAs for $Al_xGa_{1-x}As$ in Fig.1(a), AlN for $Al_xGa_{1-x}N$ in Fig.1(c) and ZnSe for $Cd_xZn_{1-x}Se$ in Fig.1(b), respectively.

For ease of representation, we have also illustrated the energies of the exciton–polaritons as functions of the composition x in the TMCs $Al_xGa_{1-x}As$, $Cd_xZn_{1-x}Se$ and $Al_xGa_{1-x}N$ for $k = 4$ and 30 in Figs.2(a) and 2(b) respectively. It is obvious that the energies of two branches of exciton–polaritons increase non-linearly with the increase of the mole fraction of the Al-components in the $Al_xGa_{1-x}As$ and $Al_xGa_{1-x}N$ systems and Zn-composition $(1 - x)$ in the $Cd_xZn_{1-x}Se$ system. The nonlinear property of the dispersion curves of exciton–polaritons originates mainly from the parabolic behaviour of the energies of exciton in TMCs. It is also concluded that the polariton energies increase with the mole fraction of the wider-gap end-material, say, AlAs, AlN and ZnSe.

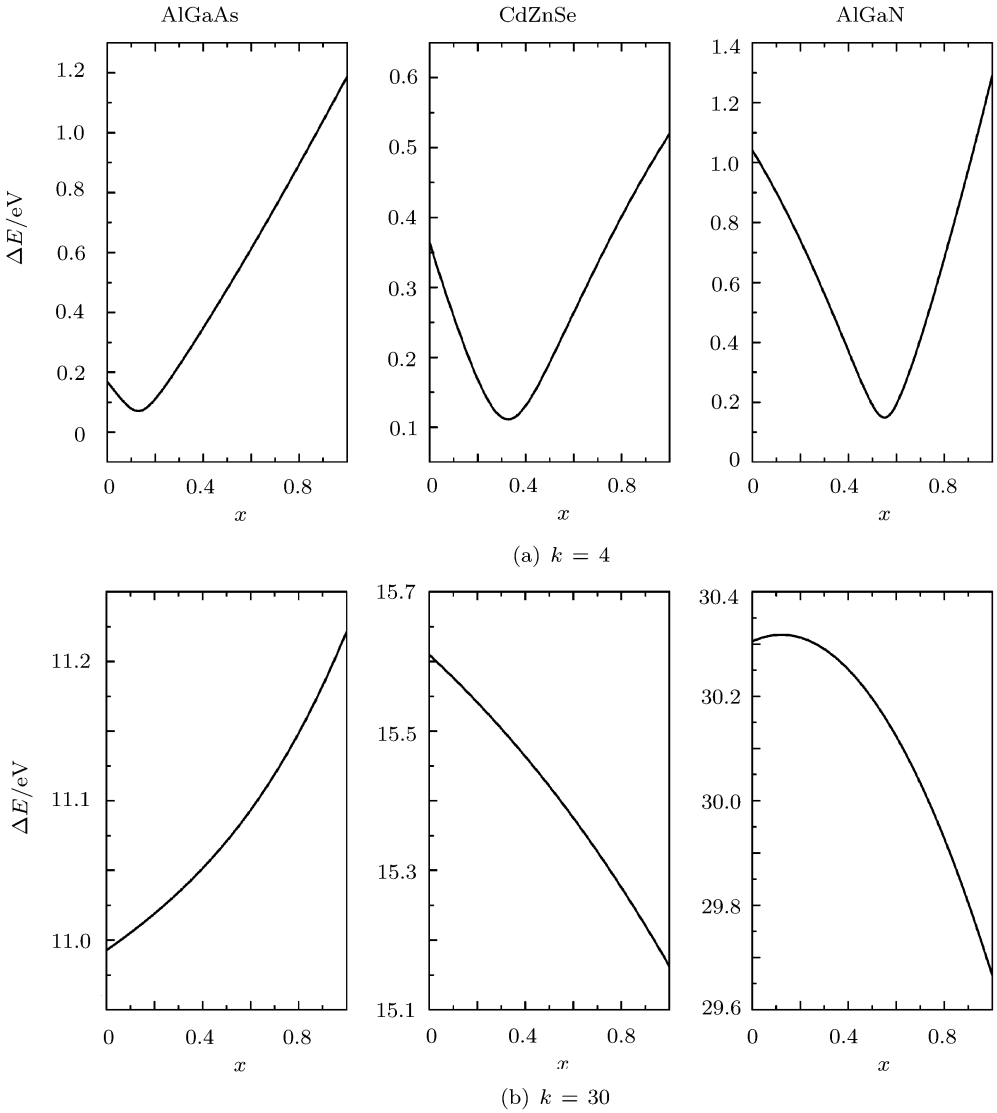


Fig.3. Splitting energies of the two branches of exciton–polaritons as functions of the composition x in the TMCs $Al_xGa_{1-x}As$, $Cd_xZn_{1-x}Se$, and $Al_xGa_{1-x}N$ for (a) $k = 4$ and (b) $k = 30$. The wave-vector k is measured in ω_{TGaAs}/c, ω_{TCdSe}/c, and ω_{TGaN}/c respectively.

Moreover, the splitting energies of the two branches of exciton–polaritons as functions of the composition x in the TMCs $Al_xGa_{1-x}As$, $Cd_xZn_{1-x}Se$, and $Al_xGa_{1-x}N$ are illustrated in Figs.3(a) and 3(b) for $k = 4$ and 30 respectively. It is found that the splitting energy is also sensitive to the composition x of TMCs. The non-linearity of the splitting with the composition x is obvious and the tendency to go up or down is related to the wave-vector k. Naturally, the exciton–polariton frequencies are rather complicated functions of the composition x as well as the wave-vector k because of the nonlinear dependences of E_g and the dispersions of the longitudinal and transverse excitons. It is clearly

seen in Figs.2 and 3 that the compositional effect on the two branches of the polariton energies and their splitting for the smaller wave-vector ($k = 4$) near the exciton-photon resonant region is much more obvious than that for the larger one ($k = 30$). The splitting has a minimum at a certain value of the composition x, where the separation of the longitudinal-transverse frequencies of excitons is reduced due to the competition between two alloy components.

4. Conclusion

We have investigated theoretically the bulk exciton–polaritons of TMCs in the Born–Huang approximation. The energies and splitting of the two branches of bulk exciton–polaritons have been calculated. The results show the new dispersion characteristics for exciton–polaritons in TMC systems in comparison with binary crystals. The appearance of the dispersion curve, the excitation energy of exciton–polaritons and the energy splitting are all sensitive to the composition of TMCs. The calculated results for some TMC systems, such as $Al_xGa_{1-x}As$ as well as GaAs, ZnSe and CdSe are in agreement with the reported experimental results. More experimental results for TMCs are expected in the future.

It is pointed out that the ternary mixed crystal $Al_xGa_{1-x}N$ has been considered as isotropic in the present work for simplicity, but without losing the qualitative validity. In fact, III-nitride compounds usually grown in a wurtzite structure is not of a cubic lattice. The further work by taking the anisotropy into account will be done in the future.

References

[1] Hopfield J J 1958 *Phys. Rev.* **112** 1555
[2] Hopfield J J and Thomas D G 1963 *Phys. Rev.* **132** 563
[3] Ulbrich R G and Weisbuch C 1977 *Phys. Rev. Lett.* **38** 865
[4] Wei W 2006 *Chin. Phys.* **15** 2600
[5] Zhang Y, Dalpian G M, Fluegel B, Wei S H, Mascarenhas A, Huang X Y, Li J and Wang L W 2006 *Phys. Rev. Lett.* **96** 026405
[6] Laussy F P, Shelykh I A, Malpuech G and Kavokin A 2006 *Phys. Rev.* B **73** 035315
[7] Liu W K, Lin S M and Zhang C S 2002 *Acta Phys. Sin.* **51** 2052 (in Chinese)
[8] Mita T, Sotome K and Ueta M J 1980 *J. Phys. Soc. Jpn.* **48** 496
[9] Nozue Y J 1982 *J. Phys. Soc. Jpn.* **51** 1840
[10] Saba M, Quochi F, Ciuti C, Oesterle U, Staehli J L, Deveaud B, Bongiovanni G and Mura A 2000 *Phys. Rev. Lett.* **85** 385
[11] Prineas J P, Ell C, Lee E S, Khitrova G, Gibbs H M and Koch S W 2000 *Phys. Rev.* B **61** 13863
[12] Semjonow A J and Pohl U W 1999 *Phys. Stat. Sol.* (b) **215** 275
[13] Komori K, Hayes G, Okada T, Deveaud B, Wang X L, Ogura M and Watanabe M 2002 *Jpn. J. Appl. Phys.* **41** 2660
[14] Fryar J, McGlynn E, Henry M O and Mosnier J P 2005 *Nanotechnology* **16** 2625
[15] Schumacher S, Czycholl G, Jahnke F, Kudyk I, Wischmeier L, Rückmann I, Voss T, Gutowski J, Gust A and Hommel D 2005 *Phys. Rev.* B **72** 081308
[16] Cronenberger S, Soleimani H R, Ostatnický T, Crégut O, Gallart M, Gilliot P and Hönerlage B 2006 *J. Phys.: Condens. Matter* **18** 315
[17] Richard M, Kasprzak J, André R, Romestain R, Dang L S, Malpuech G and Kavokin A 2005 *Phys. Rev.* B **72** 201301
[18] Liang X X and Ban S L 2004 *Chin. Phys.* **13** 71
[19] Nepal N, Li J, Nakarmi M L, Lin J Y and Jiang H X 2006 *Appl. Phys. Lett.* **88** 062103
[20] Seisyan R P, Kosobukin V A, Vaganov S A, Markosov M A, Shamirzaev T S, Zhuravlev K S, Bakarov A K and Toropov A I 2005 *Phys. Stat. Sol.* (c) **2** 900
[21] Sugisaki M, Ren H W, Nishi K, Sugou S and Masumoto Y 2000 *Phys. Rev.* B **61** 16040
[22] Bigenwald P, Nikolaev V V, Solnyshkov D, Kavokin A, Malpuech G and Gil B 2004 *Phys. Rev.* B **70** 205343
[23] Shelykh I, Kavokin K V, Kavokin A V, Malpuech G, Bigenwald P, Deng H, Weihs G and Yamamoto Y 2004 *Phys. Rev.* B **70** 035320
[24] Huang R, Yamamoto Y, André R, Bleuse J, Muller M and Ulmer-Tuffigo H 2002 *Phys. Rev.* B **65** 165314
[25] Tilley D R 1980 *J. Phys.* C **13** 781
[26] Sell D D, Stokowski S E, Dingle R and Dilorenzo J V 1973 *Phys. Rev.* B **7** 4568
[27] Sturge M D 1962 *Phys. Rev.* **127** 768
[28] Seraphin B O 1976 *Optical Properties of Solid-New Development* ed Hamakawa Y and Nishino T (Amsterdam: North-Holland) p256
[29] Hopfield J J and Thomas D G 1960 *J. Phys. Chem. Solids* **12** 276
[30] Rashba E I and Sturge M D 1982 *Modern Problems in Condensed Matter Sciences* ed Agranovich V M and Maradudin A A (New York: North-Holland) p14
[31] Adachi S 1985 *J. Appl. Phys.* **58** R1
[32] Bosio C, Staehli J L, Guzzi M, Burri G and Logan R A 1988 *Phys. Rev.* B **38** 3263
[33] Kartheuser E 1972 *Polarons in Ionic Crystals and Polar Semiconductors* ed Devreese J T (Amsterdam: North-Holland) p718
[34] Cingolani R, Prete P, Greco D, Giugno P V, Lomascolo M, Rinaldi R, Calcagnile L, Vanzetti L, Sorba L and Franciosi A 1995 *Phys. Rev.* B **51** 5176
[35] Wang H, Farias G A and Freire V N 1999 *Phys. Rev.* B **60** 5705
[36] Pearah P J, Masselink W T, Klem J, Henderson T, Morkoc H, Litton C W and Reynolds D C 1985 *Phys. Rev.* B **32** 3857
[37] Tamargo M C 2002 *II-VI Semiconductor Materials and Their Applications* (New York: Taylor and Francis) p132
[38] Sermage B and Fishman G 1981 *Phys. Rev.* B **23** 5107
[39] Hermann C and Yu Peter Y 1980 *Phys. Rev.* B **21** 3675